

Nopp140 Functions as a Molecular Link Between the Nucleolus and the Coiled Bodies

Cynthia Isaac, Yunfeng Yang, and U. Thomas Meier

Department of Anatomy and Structural Biology, Albert Einstein College of Medicine, Bronx, NY 10461

Abstract. Coiled bodies are small nuclear organelles that are highly enriched in small nuclear RNAs, and that have long been thought to be associated with the nucleolus. Here we use mutational analysis, transient transfections, and the yeast two-hybrid system to show that the nucleolar phosphoprotein Nopp140 functions as a molecular link between the two prominent nuclear organelles. Exogenous Nopp140 accumulated in the nucleolus rapidly, but only after a lag phase in coiled bodies, suggesting a pathway between the two organelles. The expression of partial Nopp140 constructs exerted dominant negative effects on the endogenous Nopp140 by chasing it and other antigens that were common to both organelles out of the nucleolus. The alternating positively and negatively charged repeat domain of

Nopp140 was required for targeting to both organelles. In addition, partial Nopp140 constructs caused formation of novel structures in the nucleoplasm and, in the case of the conserved carboxy terminus, led to the dispersal of coiled bodies. As a final link, we identified the coiled body-specific protein p80 coilin in a yeast two-hybrid screen with Nopp140. The interaction of the two proteins was confirmed by coimmunoprecipitation. Taken together, Nopp140 appeared to shuttle between the nucleolus and the coiled bodies, and to chaperone the transport of other molecules.

Key words: nucleolus • coiled bodies • protein transport • protein interaction • transfection

THE nucleoplasm is highly compartmentalized despite the absence of separating membranes. The most conspicuous compartment is the nucleolus, where ribosomal RNA is transcribed, processed, and assembled into preribosomal particles together with ribosomal proteins. Other nuclear domains include the interchromatin granule clusters, the perichromatin fibrils, and a host of nuclear bodies that can be distinguished on an EM level or by immunofluorescent labeling of specific marker proteins (for review see Brasch and Ochs, 1992; Spector, 1993; Strouboulis and Wolffe, 1996). Most of these subnuclear compartments are highly dynamic structures whose size, shape, and location constantly change according to metabolic activities. In addition, several of these compartments appear functionally linked, and communicate with each other. In particular, the nucleolus and the coiled bodies have been associated with each other by scientists for close to 100 yr (Ramón y Cajal, 1903; Hardin et al., 1969; Raska et al., 1990).

Coiled bodies were initially identified on the light microscopic level in 1903 as accessory bodies of the nucleolus,

and were later rediscovered on the EM level as coiled bodies (Ramón y Cajal, 1903; Hardin et al., 1969; Monneron and Bernhard, 1969). The major insight into their molecular composition came with the identification of the coiled body-specific protein p80 coilin, whose function remains to be determined (Andrade et al., 1991; Raska et al., 1991). Coiled bodies harbor mainly three classes of small nuclear RNPs (snRNPs),¹ which are involved in pre-mRNA splicing, preribosomal RNA processing, and histone pre-mRNA 3'-end formation (for review see Bohmann et al., 1995a). It has, however, been demonstrated that none of the target RNAs of these snRNPs are present in coiled bodies. Therefore, it appears that coiled bodies function in the storage or the biogenesis of these snRNPs. Not only is the latter possibility more attractive, but it is also analogous to the function of another prominent nuclear organelle, the nucleolus, which forms large RNPs, the ribosomes. Interestingly, there are several other connections between the nucleolus and the coiled bodies. Coiled bodies are often located in the vicinity of nucleoli, or are physically attached to them, seemingly emerging from or fusing with them (Hardin et al., 1969; Lafarga et al., 1983;

Address all correspondence to Thomas Meier, Department of Anatomy and Structural Biology, Albert Einstein College of Medicine, 1300 Morris Park Avenue, Bronx, NY 10461. Tel.: 718-430-3294; Fax: 718-430-8996; E-mail: meier@aecom.yu.edu

1. *Abbreviations used in this paper:* GFP, green fluorescent protein; HA, hemagglutinin; NLS, nuclear localization signal; snoRNP, small nucleolar RNP; snRNP, small nuclear RNP.

Ferreira and Carmo-Fonseca, 1995). In some cases, coiled bodies are even found within nucleoli (Malatesta et al., 1994; Ochs et al., 1994; Lyon et al., 1997). Physically and structurally, the coiled bodies are most closely associated with the dense fibrillar component of the nucleolus (Hardin et al., 1969; Lafarga et al., 1983). Nucleoli and coiled bodies also share several macromolecules; in particular, components of small nucleolar RNPs (snoRNPs) such as fibrillarin (Reimer et al., 1987), NAP57 (unpublished result; Meier and Blobel, 1994), and U3 small nucleolar RNA. In addition, topoisomerase I, ribosomal protein S6, and Nopp140 are present in both organelles (Raska et al., 1991; Jiménez-García et al., 1994; Meier and Blobel, 1994). Finally, a functional interaction of coiled bodies and the nucleolus was suggested by the negative effects of partial p80 coilin constructs on the structure of the nucleolus (Bohmann et al., 1995b). Despite this wealth of evidence for an association between these two nuclear organelles, little is known about its molecular basis.

Likely candidates providing the molecular basis for a nucleolar-coiled body interaction are the molecules shared by both organelles; in particular, fibrillarin, NAP57, and Nopp140, which are all constituents of the coiled body-related dense fibrillar component of the nucleolus. Fibrillarin and its yeast ortholog Nop1p are essential components of box C/D snoRNPs, which are involved in processing and ribose methylation of ribosomal RNA (Tollervey et al., 1993; Kiss-Lászó et al., 1996; Nicoloso et al., 1996). NAP57 and its yeast ortholog Cbf5p are part of the box H/ACA snoRNPs required for pseudouridylation of ribosomal RNA (unpublished results; Ganot et al., 1997; Lafontaine et al., 1998). The function of Nopp140, however, remains to be determined, although we proposed it to be involved in the assembly and/or transport of preribosomal subunits. Nopp140 shuttles between the nucleolus and the cytoplasm, apparently on tracks observed by immuno EM (Meier and Blobel, 1992). Unlike most other nucleolar proteins, Nopp140 lacks RNA-binding motifs or glycine/arginine-rich stretches. It exhibits a three-domain structure, the unique and evolutionarily conserved amino and carboxy termini, and the signature central repeat domain. The repeat domain contains ten acidic serine clusters alternating with exclusively basic stretches rich in lysine, alanine, and proline residues. Most of the serine residues in the acidic clusters are phosphorylated by casein kinase 2, rendering Nopp140 one of the most highly phosphorylated proteins in the cell with up to 82 phosphates/molecule. This negative and positive charge density may serve to neutralize charges, on one hand on proteins associated with Nopp140, and on the other on nuclear chromatin and RNPs, thereby allowing smooth passage of Nopp140 and attached molecules (Meier and Blobel, 1992; Meier and Blobel, 1994). The very carboxy terminus of Nopp140 is phylogenetically most highly conserved, exhibiting 59% sequence identity with its yeast homolog Srp40p (Meier, 1996). Such a high degree of conservation suggests a conserved function for Nopp140.

Here we present evidence that Nopp140 not only moves between the nucleolus and the cytoplasm, but also between the nucleolus and the coiled bodies. Exogenous expression of the conserved carboxy terminus of Nopp140 exerts a dominant negative effect on endogenous Nopp140. It disperses

coiled bodies and chases specifically those antigens out of the nucleolus that are common to coiled bodies. We demonstrate that Nopp140 not only associates with nucleolar proteins, but also interacts with p80 coilin of the coiled bodies. Taken together, these data suggest Nopp140 as a dynamic link between the nucleolus and the coiled bodies.

Materials and Methods

DNA Constructs

Cloning was in general performed according to standard techniques (Maniatis et al., 1989). Unless otherwise stated, inserts with appropriate restriction sites were amplified by PCR using the hot-start technique to avoid false priming. The constructs were confirmed by restriction analysis or by sequencing of the newly generated linkers.

Mammalian Expression Constructs

The mammalian expression vectors either had an SV40 early (pSVK3; Pharmacia Biotech, Inc., Piscataway, NJ) or late promoter (pSVL; Pharmacia Biotech, Inc.). Full-length Nopp140 was tagged with a double hemagglutinin (HA)-tag by cloning amplified Nopp140 into pTM27 while dropping out SRP40, thus generating pTM37. HA-Nopp140 in pET22b (Novagen, Inc., Madison, WI). pTM27 was constructed by subcloning a double HA-tag and SRP40 into pET22b (Novagen, Inc.). HA-Nopp140 under the control of the SV40 late promoter (pTM40) was generated by subcloning HA-Nopp140 from pTM37 into pSVL (Pharmacia Biotech, Inc.). Similarly, HA-Nopp Δ Cb under the control of the SV40 early promoter (pTM38) was created by subcloning from pTM37 into pSVK3 (Pharmacia Biotech, Inc.). To generate HA-Nopp140 under the control of the SV40 early promoter (pTM93), NoppCb was cloned from pTM37 into pTM38.

The HA-tagged Nopp140 deletion constructs were all generated initially in pACT2 (CLONTECH Laboratories, Inc., Palo Alto, CA) for two-hybrid analysis. From those vectors, the constructs were excised using Bgl II, and were cloned into that site of pSVM that we constructed by inserting synthetic oligonucleotides (containing a strong Kozak initiation codon followed by a Bgl II site) into pSVL (Pharmacia Biotech, Inc.). Therefore, the following constructs were all under the control of the SV40 late promoter: HA-Nopp Δ C (pWG7), HA-Nopp Δ N (pWG15), HA-NoppN (pWG10), HA-NoppR (pWG14), HA-NoppC (pWG13), HA-NoppCa (pWG17), HA-NoppCb (pWG16), HA-Nopp Δ Cb (pWG21), and HA-Nopp140 (pWG12).

Green fluorescent protein (GFP)-nuclear localization signal (NLS) expression constructs were made by amplifying GFP using pGreenLantern™ (CLONTECH Laboratories, Inc.) as template and a 3'-primer encoding the NLS of SV40 large T antigen (Kalderon et al., 1984; Lanford and Butel, 1984), and cloning it into pSVK3 (Pharmacia Biotech, Inc.), generating pGFPNLS. HA-tagged Nopp140 constructs were then cloned as described for the deletion constructs above from pACT2 (CLONTECH Laboratories, Inc.) into pGFPNLS creating GFP-NLS-HA-NoppN (pTM101), GFP-NLS-HA-NoppC (pTM103), GFP-NLS-HA-NoppCa (pTM99), and GFP-NLS-HA-NoppCb (pTM97).

Two-hybrid Constructs

LexA DNA binding and GAL4 activation domain (GAD) fusion proteins were constructed by subcloning the respective amplified Nopp140 fragments into pBTM116 (Bartel et al., 1993) and pACT2 (CLONTECH Laboratories, Inc.). Thus, the following constructs were generated: LexA-Nopp140 (pSY1), GAD-Nopp140 (pTM47), GAD-Nopp Δ Cb (pTM67), GAD-Nopp Δ C (pTM68), GAD-NoppN (pTM66), GAD-NoppR (pTM63), and GAD-NoppC (pTM73). The LexA-p80 coilin 1–186 (pYY9) was constructed by subcloning p80 coilin (amino acid 1–186) from the original two-hybrid isolate, p2HY1, into pBTM116. The other isolate was GAD-p80 coilin (amino acid 1–161), p2HY12.

Transient Transfections

Mostly COS-1 cells, but also HeLa and NIH 3T3 fibroblasts grown in DMEM (Gibco Laboratories, Grand Island, NY) supplemented with 10% FBS (Gibco Laboratories) were used for the transfection studies. The cells were transiently transfected by the calcium phosphate (Chen and Okyama, 1987) or DEAE dextran method (McCutchan and Pagano,

1968). Both methods yielded identical results and exhibited efficiencies of 5–30% depending on the construct. The DNA constructs were purified over QIAGEN columns (QIAGEN, Inc., Chatsworth, CA) for transfection. The length of transfection was determined by the promoter of the transfected construct, and was usually 48 h with the SV40 late promoter constructs unless otherwise stated. The described phenotypes were observed in at least 80% of the transfected cells unless specified.

Immunochemical Methods

For indirect immunofluorescence analysis, cells were grown on coverslips, and were fixed and permeabilized with formaldehyde (EM Science, Gibbstown, NJ) and Triton X-100 (Bio-Rad Laboratories, Hercules, CA), respectively (Meier and Blobel, 1990). Antigens were detected by incubation with primary antibodies followed by secondary antibodies labeled with fluorochromes. The following primary antibodies were used at the dilutions given in parentheses: anti-recombinant Nopp140 serum (RH10 at 1:1,000; Meier, 1996), anti-Nopp140 peptide serum (RF11 at 1:1,000; Meier and Blobel, 1992), anti-HA ascites fluid (12CA5 at 1:200; Wilson et al., 1984), anti-p80 coilin ascites fluid (5P10 at 1:10,000; from Maria Carmo-Fonseca, Lisbon, Portugal), anti-p80 coilin polyclonal antiserum (204/10 at 1:500; Bohmann et al., 1995b), anti-recombinant NAP57 rabbit serum (RP7 at 1:200; raised against recombinant NAP57 as previously described for Nopp140; Meier, 1996), anti-fibrillarin monoclonal IgGs (D77 at 1 µg/ml; Aris and Blobel, 1988), anti-nucleolin ascites fluid (7G2 at 1:2,000; from Serafin Pinol-Roma, Mount Sinai Medical Center, New York), anti-B23/NO38 IgG (B23 C-19 at 0.4 µg/ml; Santa Cruz Biotechnology, Santa Cruz, CA), anti-RNA polymerase I serum (αPolIβ at 1:50; from Larry Rothblum, Geisinger Clinic/Weis Center for Research, Danville, PA), anti-UBF serum (αUBF at 1:100; from Larry Rothblum), and anti-Sm ascites fluid (Y12 at 1:1,000; Lerner et al., 1981). Secondary antibodies were usually rhodamine-labeled goat anti-rabbit IgG and FITC-labeled goat anti-mouse IgG antibodies, both from Boehringer Mannheim Corp. (Indianapolis, IL), or in the case of B23/NO38 IgG, donkey anti-goat IgG (FITC) and donkey anti-mouse IgG (Texas red), both from Jackson ImmunoResearch Laboratories (West Grove, PA). Immunofluorescence was observed with an IX70 inverted microscope (Olympus America Inc., Melville, NY), collected with a PXL-cooled CCD camera (Photometrics, Tuscon, AZ), and processed using IPLab software (Signal Analytics Corporation, Vienna, VA). The pictures were prepared for publication as previously described (Meier, 1996). Fluorescence intensities were quantitated using National Institutes of Health image software.

For Western blots, entire 10-cm dishes were transfected, the cells were scraped into ice-cold PBS, washed twice, and lysed in SDS sample buffer by tip sonication. SDS-PAGE, transfer to nitrocellulose, and immunodetection were performed as described (Meier, 1996).

Yeast Two-Hybrid Analysis

The yeast strains used were L40 (*Mata his3Δ200 trp1-901 leu2-3, 112ade2 LYS::[lexAop]_r-HIS3 URA3::[lexAop]_s-lacZ*) and L41 (*Mata his3Δ200 trp1-901 leu2-3, 112ade2 LYS::[lexAop]_r-HIS3 URA3::[lexAop]_s-lacZ*; Hollenberg et al., 1995). Yeast cell culture, genomic DNA preparation, and general manipulations were performed essentially as described (Ausubel et al., 1993). To screen for Nopp140-interacting proteins, an L40 strain carrying pSY1, SYY1, was transformed with a HeLa two-hybrid library (Hannon et al., 1993). An estimated 5×10^6 clones were screened for growth on medium lacking histidine, and the 90 growing colonies were tested for β-galactosidase activity using a filter assay (Breedon and Nasmyth, 1985). The plasmid DNA was isolated from the 27 remaining colonies, electroporated into *Escherichia coli*, isolated, and retransformed into yeast L41, which were mated with SYY1 and tested for activation of the HIS3 and lacZ gene as described above. Of the 13 plasmids that still transactivated the reporter genes, 6 were identified by DNA sequencing as the amino terminus of p80 coilin. To quantitate the β-galactosidase activity, liquid assays were performed essentially as described (Guarente, 1983). The average value of two separate experiments with three individual transformants for each set is reported. The values from individual transformants differed <20% from the average value.

In Vitro Transcription/Translation and Immunoprecipitations

The following plasmids were used for in vitro transcription/translation in a coupled reticulocyte lysate system (Promega Corp., Madison, WI): pYY23, pBluescript II SK⁺ (Stratagene, La Jolla, CA) carrying full-length p80 coi-

lin amplified from a plasmid provided by Chung-Hsiun Herbert Wu (Medical School, National Taiwan University, Taipei, Taiwan), and pLAM-2, pBluescript II SK⁺ (Stratagene) carrying full-length human lamin B (Pollard et al., 1990). The proteins were transcribed/translated according to the description of the manufacturer and labeled with [³⁵S]methionine and -cysteine using Express™ label from DuPont-NEN (Boston, MA). For coimmunoprecipitation experiments, recombinant Nopp140 (0.5 µg; Meier, 1996) was added to the in vitro-translated protein and precipitated with 2 µg of anti-Nopp140 peptide IgGs in the presence or absence of a 100-fold molar excess of free peptide. Precipitations were performed as described (Meier and Blobel, 1994), except that SDS was omitted from all the buffers. The precipitated proteins were analyzed by SDS-PAGE, followed by Coomassie blue stain and fluorography with Enlightning™ (DuPont-NEN).

Results

Nopp140 Targeting to the Nucleolus and the Coiled Bodies

To study nucleolar and coiled body targeting of Nopp140, we amino-terminally tagged Nopp140 constructs with the HA epitope, and transfected them into COS-1 cells. As observed by indirect immunofluorescence, full-length HA-Nopp140, expressed from the SV40 early promoter, accumulated in nucleoli 6–12 h after transfection (Fig. 1, compare *a* with *a'*). Its pattern was indistinguishable from that of endogenous Nopp140 (see Fig. 4 *a'*). Unlike the endogenous Nopp140, however, it did not concentrate in coiled bodies identified by the coiled body marker protein p80 coilin (Fig. 1, compare *a* with *a''*). Only 12 h later was transfected HA-Nopp140 observed in coiled bodies (see Fig. 1 *b*). This lag phase of coiled body accumulation was independent of cell type and promoter used to express Nopp140 because it was also observed in HeLa and NIH 3T3 cells, and with both the SV40 early and late promoter (data not shown). In the case of the SV40 late promoter, HA-Nopp140 expression was delayed to 24 h after transfection, and its coiled body localization was only detected consistently after 48 h.

The phenotype of sequential accumulation in the two nuclear organelles could be explained by a difference in fluorescence intensities of Nopp140 in those two locations. To investigate this possibility, we quantitated the fluorescence in nucleoli and coiled bodies of untransfected cells stained with two different anti-Nopp140 antibodies. The maximal fluorescence intensities of coiled bodies corresponded closely to those of nucleoli, and in many cases even exceeded them (data not shown). Therefore, there existed a true temporal lag phase between accumulation of exogenously expressed Nopp140 in the nucleolus and in coiled bodies. Such a lag phase could also occur if the cells needed to go through mitosis, during which coiled bodies disassemble before Nopp140 can accumulate in the coiled bodies. This, however, is unlikely since we never observed transfected cells in mitosis, and since the transfected cells were usually not arranged side by side in a typical postmitotic pattern. In summary, these data demonstrate that newly synthesized Nopp140 first targets to the nucleolus and only subsequently to the coiled bodies, indicating that the way to the coiled bodies leads through the nucleolus.

Targeting and Effects of Partial Nopp140 Constructs

Separate signals in Nopp140 with different affinities for the nucleolus and the coiled bodies could account for its

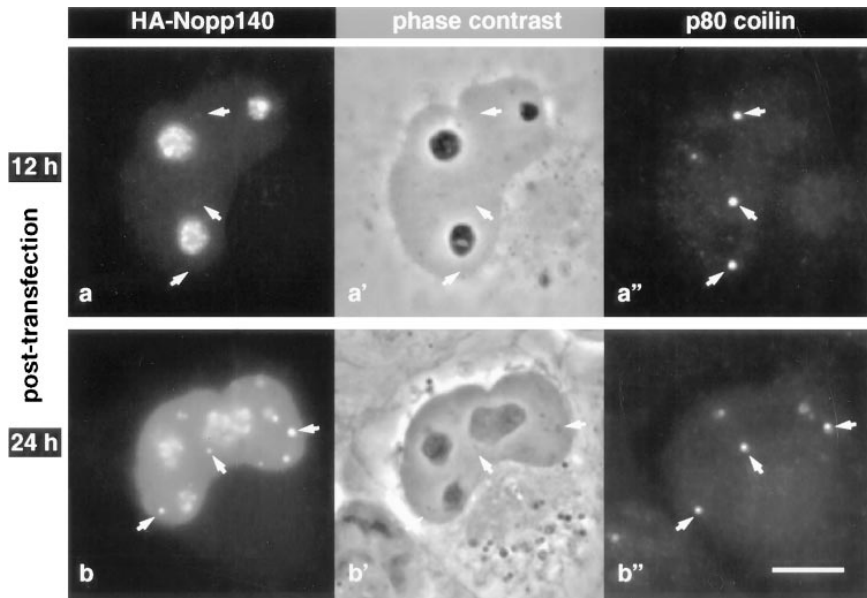


Figure 1. Exogenously expressed Nopp140 targets properly to nucleoli, but only after a lag phase to coiled bodies. The amino terminally HA-tagged cDNA of Nopp140 was transiently transfected into COS-1 cells; (a) 12 h and (b) 24 h after transfection. Exogenous Nopp140 was detected by indirect immunofluorescence with anti-HA antibodies (a and b), which was compared with phase contrast (a' and b') and double immunofluorescence with anti-p80 coilin antibodies (a'' and b''). Arrows point out some of the coiled bodies. Bar, 10 μ m.

differential localization to the nucleolus and the coiled bodies. To investigate this possibility, truncated constructs were HA-tagged, and their distribution was analyzed by indirect immunofluorescence after transient transfection (Fig. 2). The constructs were based on the three-domain structure of Nopp140, the short evolutionary conserved amino (NoppN) and carboxy termini (NoppC), and the major central repeat domain (NoppR, Fig. 3). The results from all transfection studies are summarized in Fig. 3. All constructs containing the entire repeat domain localized at least initially to the nucleolus (Fig. 2, a and b), and eventually to coiled bodies (Fig. 2 c, Fig. 5, A and C, *open arrows*). The repeat domain alone was detectable in the nucleolus only at early time points after transfection (not

shown), and became excluded from it after 48 h (Fig. 2 C). Neither the carboxy terminus (Fig. 2 D) nor the amino terminus alone (see below and Fig. 4) accumulated in the nucleolus or the coiled bodies. Therefore, the repeat domain was required for both the nucleolar and the coiled body accumulation of Nopp140.

Surprisingly, partial constructs of Nopp140 containing the repeat domain caused formation of phase-dense structures in the nucleoplasm (Fig. 2, A–C, *solid arrows*). According to their appearance by indirect immunofluorescence (Fig. 2, b' and c'), we termed these structures R-rings for NoppR-induced rings. In the case of the HA-Nopp Δ C construct (Fig. 2 a), the R-rings were often small, and at an initial state of their formation when compared

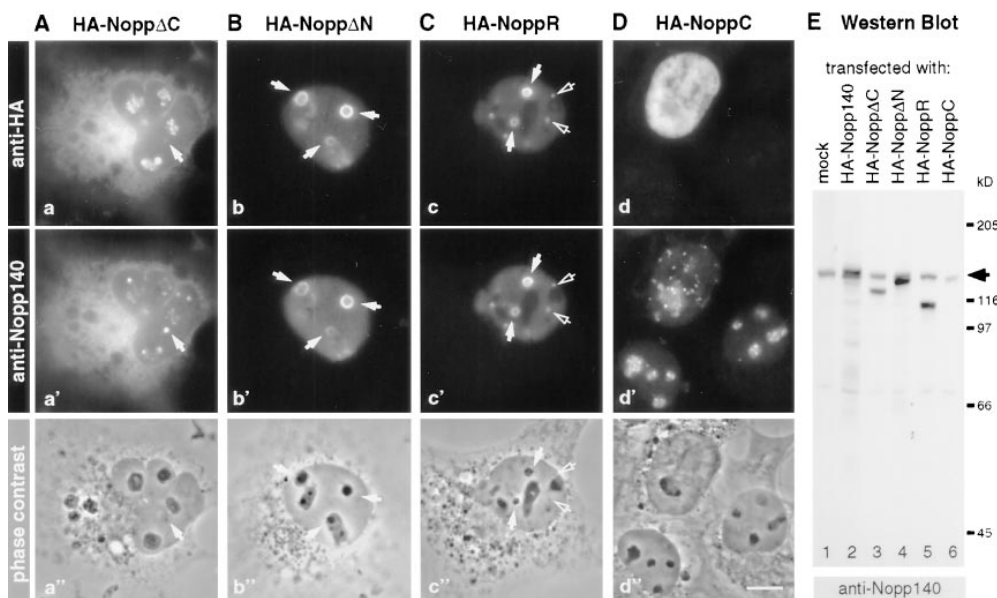


Figure 2. Effects of HA-tagged partial Nopp140 constructs transiently transfected into COS-1 cells. (A–D) The Nopp140 constructs were detected by indirect immunofluorescence with anti-HA antibodies (a–d) and compared to endogenous Nopp140 with anti-Nopp140 antibodies, which did not recognize NoppC (a'–d'). Phase contrast images of the same fields are shown as reference (a''–d''). Some R-rings (*solid arrows*) and coiled bodies (*open arrows*) are pointed out. Note in (D) that endogenous Nopp140 was only chased from the nucleoli of the transfected cell (compare d with d'). The constructs correspond to those

depicted in Fig. 3. Bar, 10 μ m. (E) Western blot of cells transfected with the constructs shown in (A–D). Endogenous Nopp140 (*arrow*) and the constructs were detected with the anti-Nopp140 antibodies, and were developed using enhanced chemiluminescence. Migrating positions of molecular weight markers are indicated on the right.

TAG-	CONSTRUCT	accumulation in					effects on	
		C	N	No	CB	RR	Nopp140	CB
	HA-Nopp140	-	-	+	+	-	-	-
	HA-NoppΔCb	-	-	+	+	-	-	-
	HA-NoppΔC	+	-	+	+	+	+	-
	HA-NoppR	-	-	+	+	+	+	-
	HA-NoppΔN	-	-	+	+	+	+	-
	HA-NoppC	-	+	-	-	-	+	+
GFP-NLS		-	+	+	-	-	-	-
GFP-NLS-HA-NoppN		+	+	-	-	-	-	-
GFP-NLS-HA-NoppC		-	+	-	-	-	+/-	+/-
GFP-NLS-HA-NoppCa		-	+	-	-	-	+/-	+/-
GFP-NLS-HA-NoppCb		-	+	-	-	-	+/-	+/-

conserved in metazoans and in yeast repeat domain (black = acidic serine clusters)

Figure 3. Summary of the transfected constructs with their properties and effects. The constructs are listed in bold, and the amino terminal tags are indicated to their left: GFP, green fluorescent protein; NLS, nuclear localization signal of SV40 large T antigen; HA, hemagglutinin epitope. Note that all constructs except GFP-NLS contain an HA tag. The schematics depict the Nopp140 constructs drawn to scale. The localization of the transfected constructs in the cytoplasm (C), nucleoplasm (N), nucleolus (No), coiled bodies (CB), and R-rings (RR) is indicated. In addition, the effects on endogenous Nopp140 (Nopp140) and coiled bodies (CB) are shown. The results were detected in most (+), almost none (-), or about half (\pm) of the transfected cells. The asterisks indicate that the localization was only observed at early time points of transfection.

with those induced by HA-NoppΔN (Fig. 2 b) and HA-NoppR (Fig. 2 c). This phenotype of HA-NoppΔC was likely caused by the lower nuclear concentration of this construct because of its considerable accumulation in the cytoplasm (Fig. 2 a). In addition to the generation of R-rings, the NoppR-containing constructs affected the localization of endogenous Nopp140. Thus, Nopp140 was recruited to the R-rings (Fig. 2, a'-c'), and was eventually excluded from the nucleolus (Fig. 2 c'). A different dominant negative effect on the endogenous Nopp140 was observed by exogenous expression of the carboxy terminus of Nopp140 alone. HA-NoppC chased endogenous Nopp140 out of the nucleolus and into nucleoplasmic granules of $\sim 0.5 \mu\text{m}$ in diameter (Fig. 2 d'). This effect appeared to occur in *trans* since HA-NoppC did not accumulate in the nucleolus, but concentrated in the nucleoplasm (Fig. 2 d). Apparently, the dominant negative effects of NoppR and NoppC adversely affected cell viability since at later time points after transfection, the number of transfected cells declined.

To ascertain that these effects were indeed caused by the intact constructs and not proteolytic fragments thereof, cells transfected with the respective constructs were analyzed by SDS-PAGE and Western blotting (Fig. 2 E). The exogenously expressed constructs could not be detected with anti-HA antibodies, although they were recognized well by those antibodies in indirect immunofluorescence experiments. This was most likely a matter of sensitivity since the same antibodies detected HA-tagged Srp40p on Western blots when uniformly expressed in yeast (Meier, 1996). Therefore, we used anti-Nopp140 antibodies that detected the endogenous and the transfected proteins simultaneously (Fig. 2 E). All constructs migrated as a sin-

gle homogeneous band at their predicted positions, indicating that none of the proteins was subject to degradation (Fig. 2 E). In addition, the relative mobility of the various Nopp140 constructs containing NoppR indicated that these exogenous constructs were fully and homogeneously phosphorylated to their exceptional high degree (Meier and Blobel, 1992; Meier, 1996). Given the transfection efficiency and the amount of exogenous protein compared with that of endogenous Nopp140, all of the constructs were overexpressed at least 10-fold. However, this value may be an overestimate since the antibodies did not recognize the COS cell Nopp140 as well as they did the rat constructs. Since these antibodies, raised against recombinant Nopp140, failed to react with the carboxy terminus of Nopp140 (data not shown and Meier, 1996), the HA-NoppC construct alone was not recognized (Fig. 2 E, lane 6).

A Nuclear Export Signal in the Amino Terminus of Nopp140

Expression of the amino terminus of Nopp140 alone could not be detected by indirect immunofluorescence with anti-HA antibodies (not shown), indicating a susceptibility of the 59-amino acid peptide to proteolysis. To stabilize the short construct, we added an amino terminal fusion protein consisting of GFP linked to the nuclear localization signal (NLS) of SV40 large T antigen (see Fig. 3; Kalderon et al., 1984; Lanford and Butel, 1984). The nuclear localization signal was added because no NLS appeared to be present in the sequence of NoppN (Meier and Blobel, 1992). This construct was expressed and localized to the nucleoplasm as well as the cytoplasm, but failed to concentrate in nucleoli or coiled bodies (Fig. 4 a). Unlike exogenous HA-NoppR and HA-NoppC, expression of GFP-NLS-HA-NoppN left the endogenous Nopp140 unaffected (Fig. 4 a'). When compared with the localization of the GFP-NLS tag alone (Fig. 4 b), GFP-NLS-HA-NoppN caused a nucleolar exclusion, indicating that NoppN was not involved in nucleolar targeting or retention. In addition, GFP-NLS-HA-NoppN (Fig. 4 a), unlike GFP-NLS alone (Fig. 4 b), accumulated partially in the cytoplasm independently of its level of expression. This NoppN-induced shift of the steady-state distribution from exclusively nuclear to partial cytoplasmic may be caused by its putative leucine-rich nuclear export signal, $^{14}\text{LYPLVLGFLR}^{23}$, which is similar to that of the HIV Rev protein (Fischer et al., 1995). In agreement with this idea, HA-NoppΔC, which lacked the NLS-rich NoppC domain (Meier and Blobel, 1992), exhibited partial cytoplasmic distribution (Fig. 2 a and Fig. 3) and in some instances accumulated at the nuclear envelope (unpublished results). While our results suggest that the nuclear export signal in NoppN is indeed functional, the presence of a cytoplasmic retention sequence cannot be excluded.

R-Rings

The R-rings ranged in size from $0.5\text{--}5 \mu\text{m}$, but measured on average $2 \mu\text{m}$ in diameter. Their number varied between 1 and 10 per cell, but most cells contained 2-5. Occasionally, R-rings even formed within nucleoli (Fig. 2 B). To determine whether the R-rings recruited additional proteins aside from endogenous Nopp140, indirect im-

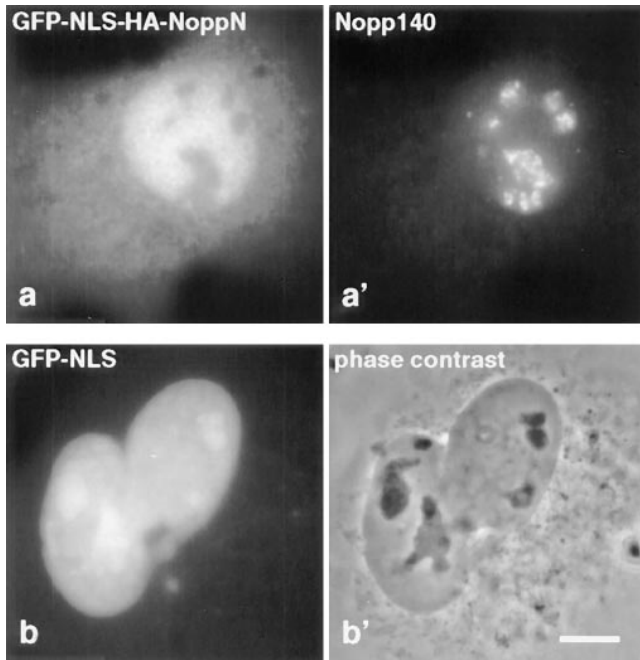


Figure 4. The nuclear export signal of NoppN appears to be functional. As visualized by immunofluorescence after transient transfection, GFP-NLS-HA-NoppN was excluded from the nucleoli, and accumulated partially in the cytoplasm (*a*), unlike the exclusively nuclear and nucleolar GFP-NLS (*b*). The GFP constructs were detected with anti-HA antibodies (*a*) or by autofluorescence (*b*), and the nuclei and nucleoli were observed with Nopp140 peptide antibodies (*a'*) or by phase contrast microscopy (*b'*) of the same field of cells. Bar, 10 μ m.

munofluorescence on HA-NoppR (Fig. 5, *A* and *B*) and HA-Nopp Δ N (Fig. 5 *C*) was performed. The R-rings also attracted or redirected fibrillarin, NAP57, the RNA polymerase I transcription factor UBF, and in part RNA polymerase I itself (Fig. 5 *A* and not shown). However, nucleolin and B23/NO38 remained completely nucleolar in transfected cells (Fig. 5 *B* and not shown). Surprisingly, the nucleolus remained intact on a light microscopic level despite the absence of these major nonribosomal nucleolar proteins, indicating that they are not essential for the phase-dense makeup of the nucleolus. Since the NoppR containing partial constructs of Nopp140 also accumulated in the coiled bodies, we tested for the presence of coiled-body antigens in the R-rings of cells transfected with NoppR-containing constructs. The coiled body marker protein, p80 coilin, was recruited to some of the R-rings (Fig. 5 *C*, *solid arrows*) but also remained in the coiled bodies (Fig. 5 *C*, *open arrows*). It is therefore possible that only p80 coilin synthesized *de novo* in the cytoplasm, but not originating from coiled bodies, was recruited to the R-rings. Other coiled-body proteins, the Sm antigens, were not recruited to the R-rings (data not shown). Sm antigens are core proteins of spliceosomal snRNPs, and concentrate in coiled bodies aside from their distribution throughout the nucleoplasm. On some occasions, R-rings were even observed in the cytoplasm (Fig. 5 *c'*), particularly when they were induced by expression of the partially cytoplasmic HA-Nopp Δ C (not shown). In summary,

the NoppR-induced R-rings recruited a subset of nucleolar antigens and depleted the nucleolus of most of these proteins while leaving its structure seemingly unaffected. In addition, p80 coilin targeted to R-rings without being depleted from coiled bodies.

Dominant Negative Effects of NoppC

As mentioned above, exogenously expressed HA-NoppC targeted to the nucleus without accumulation in the nucleolus (Fig. 2 *d*). In HA-NoppC-transfected cells, endogenous Nopp140 was chased out of the nucleolus into nucleoplasmic granular structures that could not be discerned on the light microscopic level (Fig. 2 *d'* and Fig. 6, *b'* and *b''*). These data demonstrated a clear dominant negative effect of HA-NoppC on endogenous Nopp140. To test for the specificity of this effect, we investigated the localization of other nucleolar antigens in HA-NoppC-transfected cells (Fig. 6). The transfected cells were identified by labeling of the transfected HA-NoppC (Fig. 6, *a'*, *c'*, and *d'*, *arrow*), or by the characteristic nucleoplasmic distribution of endogenous Nopp140 (Fig. 6 *b'*, *arrows*). Only NAP57 and fibrillarin were chased out of the nucleolus by HA-NoppC (Fig. 6, *a* and *b*), but not nucleolin or UBF (Fig. 6, *c* and *d*). In addition, the nucleolar localization of B23/NO38 and RNA polymerase I remained unaffected by expression of HA-NoppC (not shown). While mislocalized fibrillarin colocalized precisely with the mislocalized endogenous Nopp140 (Fig. 6 *B*; compare *b* with *b'*),

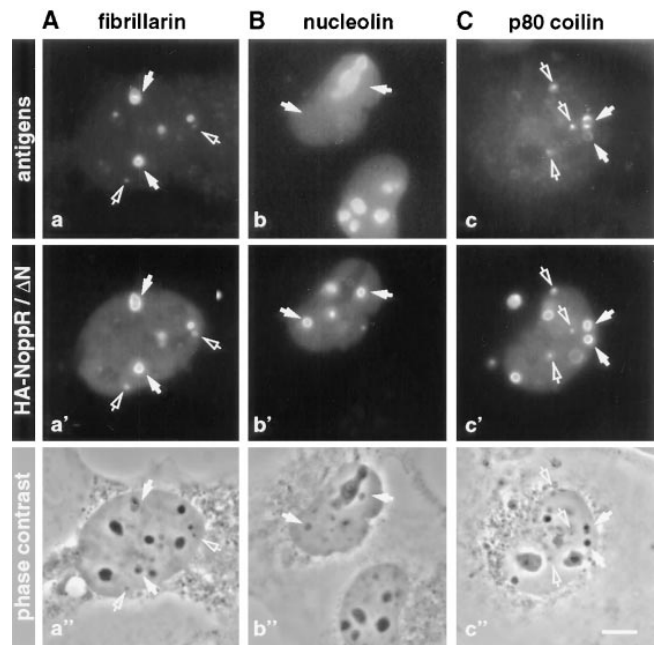


Figure 5. R-rings recruit only certain antigens. Cells were transiently transfected with NoppR (*A* and *B*) and Nopp Δ N (*C*) to induce R-rings. The localization of fibrillarin (*a*), nucleolin (*b*), and p80 coilin (*c*) was detected with the respective antibodies, and was compared by indirect double immunofluorescence with that of the transfected constructs with HA-antibodies (*a'*–*c'*) and with the phase contrast images of the same fields of cells (*a''*–*c''*). Some R-rings (*solid arrows*) and coiled bodies (*open arrows*) are pointed out. Bar, 10 μ m.

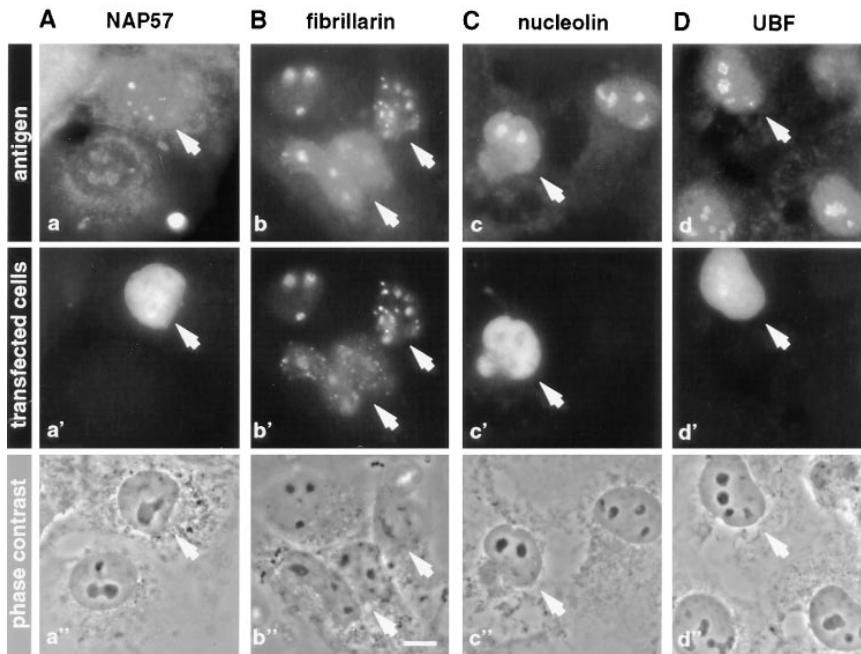


Figure 6. Exogenous expression of NoppC chases some proteins out of the nucleolus (A and B) while leaving the localization of others unaffected (C and D). NoppC-transfected cells (arrows) were detected with anti-HA antibodies (a', c', d') or by the extranucleolar localization of endogenous Nopp140, visualized with anti-Nopp140 antibodies (b'). NAP57 (a), fibrillarin (b), nucleolin (c), and UBF (d) were observed with their respective antibodies, and were compared by indirect double immunofluorescence with the transfected constructs and with the phase contrast images of the same fields of cells (a''–d''). Bar, 10 μ m.

NAP57 accumulated in a distinct pattern in the nucleoplasm of HA-NoppC-transfected cells (Fig. 6 a, arrow and not shown). Despite the loss of these antigens from the nucleolus in transfected cells, the nucleolar appearance in phase contrast remained unaffected (Figs. 6 and 7, phase contrast). This result indicated that these proteins are not essential for maintaining the structural integrity of the nucleolus. In conclusion, HA-NoppC exerted a dominant negative effect on endogenous Nopp140, and affected the localization of a few select nucleolar proteins.

These nucleolar proteins—Nopp140, NAP57, and fibrillarin—colocalized to both the nucleolus and the coiled bodies, while all the other antigens tested were exclusively nucleolar. For this reason, we investigated the effect of exogenous HA-NoppC on coiled bodies. Coiled bodies appeared disassembled in HA-NoppC-transfected cells as judged by the dispersed distribution of p80 coilin throughout the nucleoplasm (Fig. 7 A, arrow). To verify that the coiled bodies were indeed dispersed, and that not only p80 coilin was chased out of them, we tested for the localization of other proteins present in coiled bodies. The Sm antigens of the spliceosomal snRNPs are usually concentrated in coiled bodies (Fig. 7 b, open arrows) aside from their patchy distribution throughout the nucleoplasm. In HA-NoppC-transfected cells, however, Sm antigens were found only in the nucleoplasm, but were not concentrated in dots, indicating a true dispersal of coiled bodies (Fig. 7 b). Therefore, exogenous HA-NoppC not only exerted a dominant negative effect on endogenous Nopp140, but also on coiled bodies.

To determine whether these dominant negative effects of HA-NoppC could be attributed to a specific region within NoppC, cells were transfected with the amino terminal, NoppCa, or the carboxy terminal half, NoppCb, of NoppC. NoppCb corresponded to the most highly conserved part of Nopp140, and shares 59% identity to its yeast homolog, Srp40p, while NoppCa is only conserved in

metazoan homologs of Nopp140 (see Fig. 3 and Meier, 1996). Similar to our observations with HA-NoppN alone (see above), the short HA-tagged NoppCa and NoppCb could not be detected in transfected cells. Interestingly, identical negative results were obtained when we attempted to express the conserved carboxy terminus of Srp40p by itself in yeast (unpublished results). To stabilize the constructs, therefore, fusion proteins were generated with GFP-NLS as in the case of HA-NoppN. These con-

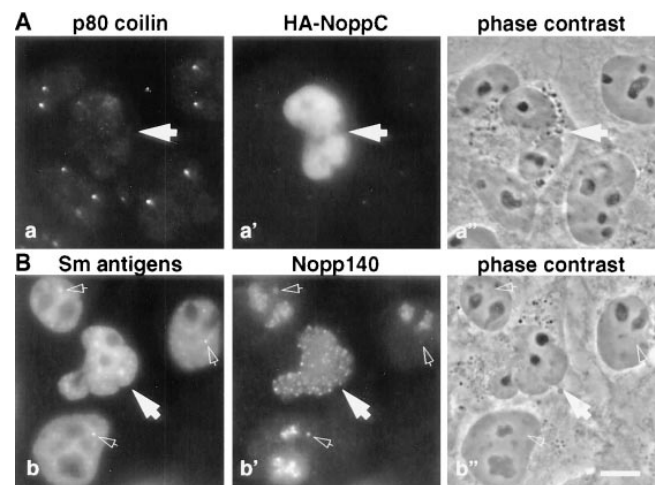


Figure 7. Exogenous expression of NoppC causes dispersion of coiled bodies as judged by the distribution of p80 coilin (A) and Sm antigens (B). NoppC-transfected cells (solid arrows) were detected with anti-HA antibodies (a') or by the extranucleolar localization of endogenous Nopp140 visualized with anti-Nopp140 antibodies (b'). p80 coilin (a) and Sm antigens (b) were observed with their respective antibodies by indirect double immunofluorescence, and were compared with the phase contrast images of the same fields of cells (a'', b''). Some coiled bodies (open arrows) in untransfected cells are indicated. Bar, 10 μ m.

structs could readily be observed in transfected cells (not shown), and the results are summarized in Fig. 3. Surprisingly, both the GFP-NLS-HA-NoppCa and -NoppCb chased endogenous Nopp140 out of the nucleolus and dispersed coiled bodies in a manner analogous to that of NoppC. These effects, however, were only observed in approximately half of the transfected cells, apparently caused by interference of the relatively large GFP-NLS-HA-tag, which accounted for >80% of the size of the NoppC constructs. This reasoning was confirmed when addition of a GFP-NLS-tag to our original HA-NoppC construct caused a similar reduction in the efficiency of its effects on endogenous Nopp140 and on coiled bodies (Fig. 3). In summary, therefore, NoppCa and NoppCb both contributed to the dominant negative effect of the entire NoppC.

This finding was in good agreement with the results obtained with NoppΔCb, the full-length Nopp140 construct lacking just NoppCb, which behaved exactly like the full-length Nopp140. Thus, HA-NoppΔCb localized to the nucleolus, but only after a lag phase to coiled bodies, and had no effects on endogenous Nopp140 or the coiled bodies (Fig. 3 and not shown). Therefore, NoppCa without NoppCb was able to provide enough functionality to the remainder of Nopp140 for its proper targeting. For full functionality, however, the highly conserved NoppCb appeared to be required as demonstrated by the dominant negative effect of GFP-NLS-HA-NoppCb alone (Fig. 3).

The Amino Terminus of p80 Coilin Interacts with Nopp140

In an independent approach, we used the yeast two-hybrid system (Fields and Song, 1989) to screen an HeLa cDNA library for Nopp140-interacting clones. Using full-length Nopp140 as bait, we identified two independent isolates of p80 coilin, one twice and the other four times. One isolate corresponded to the GAL4 activation domain fused to the first 161 amino acids, and the other the first 186 amino acids of the 576 amino acid-long p80 coilin, respectively (Fig. 8 A). Activation of reporter genes occurred whether the amino terminus of p80 coilin was fused to the GAL4 activation domain or the DNA-binding domain of LexA, indicating a true interaction with Nopp140 (Fig. 8 A). On the contrary, neither Nopp140 nor the amino terminal p80 coilin constructs exhibited any interaction with another nuclear protein, lamin B, or the GAL4 activation domain alone (Fig. 8 A). Further two-hybrid analysis to map the p80 coilin-binding site on Nopp140 revealed that the interaction was virtually lost as soon as Nopp140 was truncated of one or several of its domains, as defined in Fig. 3 (Fig. 8 A). This finding suggested that full-length Nopp140 was required, at least when fused to the GAL4 activation domain, to stabilize its tertiary structure, allowing binding of the amino terminus of p80 coilin. In the context of these findings, the amino terminus of p80 coilin failed to interact with NoppC, which exhibited the dominant negative effects on Nopp140 and the coiled bodies. Finally, it is interesting to note that the Nopp140-interacting amino terminus of p80 coilin contained the sequence that was required for its targeting to sphere organelles, the coiled body equivalent in amphibian oocytes (Wu et al., 1994).

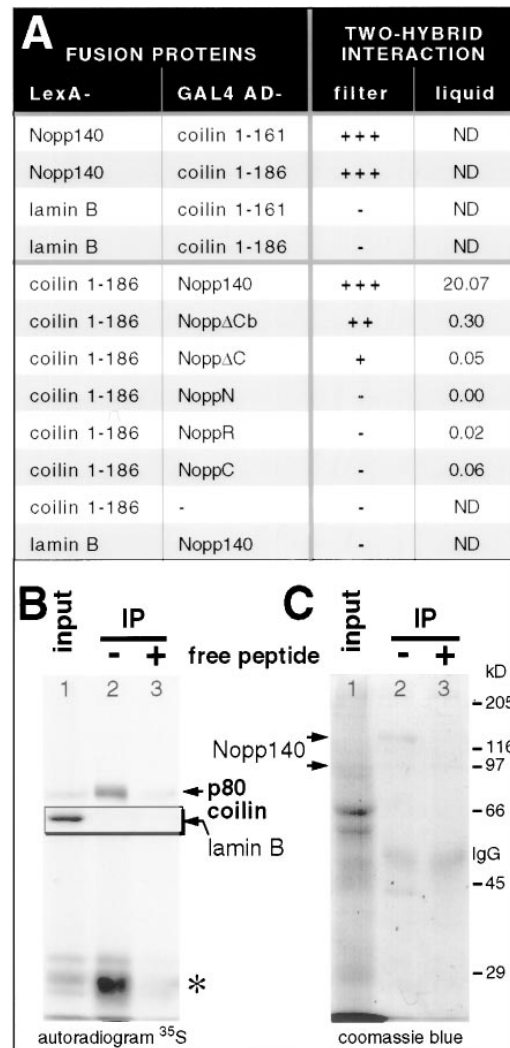


Figure 8. p80 coilin specifically interacts with Nopp140 in the yeast two-hybrid system (A), and coprecipitates with bacterially expressed Nopp140 (B and C). (A) The amino terminal 161 (coilin 1-161) or 186 amino acids of p80 coilin (coilin 1-186), lamin B, or various Nopp140 constructs as defined in Fig. 3 were fused to the DNA-binding domain of LexA (LexA-) and/or the transcriptional activation domain of GAL4 (GAL4 AD-). Their interaction was detected by their ability to transactivate β -galactosidase expression in yeast. β -galactosidase activity was determined using a filter or liquid assay as described in Materials and Methods. Blue color developed before 1/2 h (+++), before 1 h (++), after 2 h (+), or not at all (-). (B and C) p80 coilin and lamin B (*insert* in B) were in vitro-transcribed/translated in the presence of [³⁵S]-methionine and -cysteine, and were analyzed by autoradiography (B) and Coomassie blue stain (C) after SDS-PAGE (lanes 1). The in vitro-translated proteins were incubated with recombinant Nopp140, which was precipitated with Nopp140 peptide antibodies in the absence (lanes 2) or presence (lanes 3) of free competing peptide. The mobility of p80 coilin, lamin B (*insert*, from a separate experiment), and the phosphorylated and unphosphorylated Nopp140 are marked by arrows. The migrating positions of molecular weight markers and IgGs are indicated on the right. The asterisk denotes a premature termination or degradation product of p80 coilin that coprecipitates with Nopp140. Only 1/20 of the amount used for the precipitation experiments (lanes 2 and 3) was loaded in lanes 1.

To further establish the interaction of Nopp140 and p80 coilin, we added bacterially expressed Nopp140 to *in vitro*-transcribed/translated p80 coilin, and coprecipitated the proteins with anti-Nopp140 peptide antibodies (Fig. 8, *B* and *C*). Indeed, *in vitro*-transcribed/translated p80 coilin (Fig. 8 *B*, lane 1) coprecipitated with Nopp140 (Fig. 8 *B*, lane 2). However, when precipitation of Nopp140 was prevented by the presence of competing peptide, only minute amounts of p80 coilin were detected in the precipitate (Fig. 8 *B*, lane 3). Coprecipitation of p80 coilin was specific because *in vitro*-translated lamin B failed to coprecipitate with Nopp140 in a separate experiment (Fig. 8 *B*, *inset*). To confirm that the same amount of IgGs was precipitated under both conditions, the gel was stained with Coomassie blue (Fig. 8 *C*). As previously observed (Meier and Blobel, 1992; Meier, 1996) and as judged by its mobility shift from 100 to 140 kD, recombinant Nopp140 became fully phosphorylated in the reticulocyte lysate (Fig. 8 *C*, lane 2). The coprecipitating band of ~ 42 kD (Fig. 8 *C*, lane 2) was therefore most likely the α chain of casein kinase 2, which associates with Nopp140 (Li et al., 1997). Taken together with the *in vivo* colocalization of Nopp140 and p80 coilin and the dominant negative effects of NoppC on p80 coilin, these data suggest a physiologically meaningful interaction between the amino terminus of p80 coilin and full-length Nopp140.

Discussion

Ever since their discovery in 1903 as accessory bodies of the nucleolus (Ramón y Cajal, 1903), coiled bodies were thought to have a connection to the nucleolus. Here we provide several lines of evidence that Nopp140 serves as the functional link between these two nuclear organelles. First, Nopp140 is a resident protein of both the nucleolus and the coiled bodies (Meier and Blobel, 1990; Meier and Blobel, 1994). Second, the temporal lag phase between its accumulation in the nucleolus and the coiled bodies suggests that the pathway to the coiled bodies leads through the nucleolus. Third, the dominant negative effect of NoppC selectively disturbs the localization of antigens common to both organelles, and causes dispersal of coiled bodies. Fourth, Nopp140 not only interacts with nucleolar antigens (Meier and Blobel, 1994; Li et al., 1997), but also with the coiled body-specific p80 coilin. Thus, the highly phosphorylated Nopp140 with its alternating negatively and positively charged stretches might serve as chaperone for the transport of components between the nucleolus and the coiled bodies.

The observed lag phase between the accumulation of Nopp140 in the nucleolus and the coiled bodies can be interpreted in several ways. Nopp140 could be independently targeted to the coiled bodies and the nucleolus owing to separate signals of different strength. This is unlikely since the same domain of Nopp140, NoppR, is sufficient and required for its targeting to both nuclear organelles. It is possible that the turnover rates of Nopp140 differ between nucleoli and coiled bodies. This possibility is diffused, however, by our findings that NoppC chases Nopp140 out of the nucleolus and disperses coiled bodies simultaneously. Therefore, Nopp140 targets the coiled bodies through the nucleolus. Alternatively, in a kinetic

argument, it may rapidly travel through the coiled bodies to the nucleolus, and only become visible in coiled bodies as a backlog once all the sites in the nucleolus are saturated. Either model suggests a pathway for Nopp140 between the nucleolus and the coiled bodies.

Effects induced by exogenous protein expression have to be interpreted with caution, particularly if the protein is overexpressed. It is important to differentiate between specific and nonspecific consequences of the transiently expressed protein. In the case of NoppC, the effects are limited to proteins and structures that we have demonstrated to be specifically associated with endogenous Nopp140. Therefore, NoppC expression exerts a specific dominant negative effect on endogenous Nopp140. The consequences of the exogenous expression of NoppR, however, are less specific, and can be explained by a combination of mechanisms (see below).

Dominant negative effects are usually caused by competitive binding of an inactivated protein, either to its functional partner or to an essential cellular factor. Although there is some evidence that Nopp140 can oligomerize (Meier, 1996; Chen and Yeh, 1997), extensive two-hybrid analysis indicated a complete lack of interaction between two full-length Nopp140s or between full-length Nopp140 and its individual domains (data not shown). Therefore, the dominant negative effects of the highly conserved carboxy terminus of Nopp140 (NoppC) are likely due to its binding to a nuclear factor. This factor is neither NAP57 (not shown) nor p80 coilin because NoppC alone does not interact with either protein in the yeast two-hybrid system. Since NoppC itself does not accumulate in the nucleolus or in the coiled bodies (Fig. 2 *d*), it apparently binds to that factor in the nucleoplasm. There it may interfere specifically with Nopp140 movement between the nucleolus and the coiled bodies, or more generally with nucleoplasmic Nopp140 shuttling. The mislocalization of specifically those antigens common to both the nucleolus and the coiled bodies and the dispersal of the latter are therefore secondary effects. They are caused by the derailment of endogenous Nopp140 by the overexpressed NoppC. This invokes a picture of dynamic interaction between the nucleolus, the coiled bodies, and the nucleoplasm. Thus, Nopp140 binds to NAP57 and fibrillarin, and ushers them constantly through the nucleoplasm to or from the nucleolus and the coiled bodies. Once in the nucleoplasm, these proteins are unable to reenter their organelles because their usher, Nopp140, has lost its guidance. In this context it is intriguing to speculate that the nucleoplasmic factor to which Nopp140 binds with its conserved carboxy terminus might be part of the tracks along which we observed Nopp140 previously (Meier and Blobel, 1992).

We proposed Nopp140 to function as a chaperone by accompanying preribosomes through the nucleoplasm (Meier and Blobel, 1992). Interestingly, both fibrillarin (Lischwe et al., 1985) and NAP57 (unpublished results) are components of small nucleolar RNPs. Therefore, Nopp140 may serve generally as a chaperone for RNPs. The dynamic picture of the nucleolus and the coiled bodies, with snoRNPs constantly coming and going, is very reminiscent of interchromatin granule clusters that harbor spliceosomal snRNPs (for review see Spector, 1993). In

that case, splicing factors move back and forth from the interchromatin granules to the sites of active transcription and splicing in the perichromatin fibrils (Misteli et al., 1997). The dynamic aspect of snRNP accumulation in coiled bodies is further underlined by the dependence of their accumulation on ongoing transcription and translation, and on cellular growth temperature (Carmo-Fonseca et al., 1993; Lafarga et al., 1994; Rebelo et al., 1996).

The fatal effects of NoppC on coiled bodies can be explained by two mechanisms. The presence of p80 coilin, or that of NAP57 and fibrillarin is required to maintain the structural integrity of the coiled bodies. Since we showed Nopp140 to interact with p80 coilin, NoppC may affect the localization of p80 coilin in a mechanism similar to that proposed for NAP57 and fibrillarin; i.e., by derailing Nopp140 as soon as it leaves the coiled bodies. This derailment, however, would require p80 coilin to constantly move in and out of the coiled bodies, indicating that its coiled body localization simply reflects a steady-state equilibrium. Thus, p80 coilin itself may go to or through the nucleolus, thereby explaining the observed effects on the nucleolus by exogenous expression of partial p80 coilin constructs (Bohmann et al., 1995b). Interestingly, in those experiments Nopp140, unlike endogenous p80 coilin, always colocalized with the structures induced by the partial p80 coilin constructs. Hence, these effects may have been mediated through Nopp140. The second interpretation implies NAP57 and fibrillarin to be required for the integrity of the coiled bodies. Is it therefore possible that the NAP57 and fibrillarin containing snoRNPs are not only involved in the modification of ribosomal RNA, but are also involved in the modification of spliceosomal snRNAs? Consequently, do the coiled bodies indeed function in the modification of snRNAs as proposed previously (Bohmann et al., 1995a)?

The effects of the NoppR domain appear more pleiotropic and less specific than those of the NoppC domain. This may be explained by a combination of mechanisms. First, NoppR may act similarly to NoppC in that it interferes with the binding of endogenous Nopp140 to a nuclear factor. Second, the unusual high-charge density on NoppR may cause nonspecific aggregation of proteins leading to the formation of R-rings. Third, overexpression of NoppR may affect many diverse nuclear processes simply by sequestering the majority of the nuclear casein kinase 2. Such a commitment by casein kinase 2 would be required to fully phosphorylate NoppR with approximately 80 phosphates (Meier and Blobel, 1992; Meier, 1996). Overexpression of full-length Nopp140 may exhibit a less severe effect on casein kinase 2 because it retains its full complement of functional domains. However, even full-length Nopp140, when overexpressed at very high levels and for a long time, will eventually lead to the dispersal of endogenous Nopp140 from the nucleolus (not shown). It is further noteworthy that the NoppR effect is dominant over NoppC because any construct containing NoppR exhibits the NoppR and not the NoppC phenotype (Fig. 3). This fact may be due to the nucleolar and coiled body targeting capacity of NoppR, which is absent from NoppC.

The most dramatic phenotype of exogenously expressed NoppR is the generation of R-rings. The circular staining of the R-rings can be explained in two ways. On one hand,

these rings may consist of large dense aggregates of the highly charged NoppR and the sequestered antigens, thereby preventing the antibodies from penetrating into the interior. On the other hand, the circular architecture could point to a specific nuclear structure that needs to be evaluated on the EM level. Interestingly, R-rings look very similar to nuclear structures that were also induced by exogenous expression of proteins. First, expression of mutant ataxin-1, the protein mutated in spinocerebellar ataxia type 1, forms similar structures (Matilla et al., 1997; Skinner et al., 1997). Thus, R-rings could provide a model for the nuclear structures observed in the neurons of patients with that neurodegenerative disease. Second, the R-rings appear very similar to the pseudo-coiled bodies induced by exogenous expression of an amino terminal construct of p80 coilin (Bohmann et al., 1995b). Pseudo-coiled bodies and R-rings may be formed by the same mechanism since we demonstrated that the amino terminus of p80 coilin interacts with Nopp140. However, several characteristics identify these two nuclear structures as distinct entities. Unlike R-rings, pseudo-coiled bodies fail to recruit RNA polymerase I, endogenous coilin, or at later stages, fibrillarin. In addition, R-rings can grow to close to ten times the size of pseudo-coiled bodies. Finally, both organelles appear to be devoid of snRNPs, but R-rings accumulate cotransfected small nucleolar RNAs, both box C/D and H/ACA snoRNAs (unpublished results).

Our transient transfection studies provide a vivid picture of the dynamic interaction between the nucleolus and the coiled bodies. The generation of cells stably transfected with our constructs under an inducible promoter will now allow us to assess the function of Nopp140 and the coiled bodies biochemically.

We thank the following people for their generous gifts of antibodies and reagents: John Aris, Maria Carmo-Fonseca, Angus Lamond, Serafin Píñol-Roma, Larry Rothblum, Joan Steitz, and Chung-Hsiun Herbert Wu. We are grateful to Wayne Grant for constructing some of the plasmids, and to the Analytical Imaging Facility of the Albert Einstein College of Medicine for use of their equipment. We thank Susan Smith for critical reading of the manuscript.

This work was supported by National Institute of Health Grant GM50725.

Received for publication 12 May 1998 and in revised form 4 June 1998.

References

- Andrade, L.E.C., E.K.L. Chan, I. Raska, C.L. Peebles, G. Roos, and E.M. Tan. 1991. Human autoantibody to a novel protein of the nuclear coiled body: immunological characterization and cDNA cloning of p80 coilin. *J. Exp. Med.* 173:1407–1419.
- Aris, J., and G. Blobel. 1988. Identification and characterization of a yeast nucleolar protein that is similar to a rat liver nucleolar protein. *J. Cell Biol.* 107:17–31.
- Ausubel, F.A., R. Brent, R.E. Kingston, D.D. Moore, J.G. Seidman, J.A. Smith, and K. Struhl. 1993. *Current Protocols in Molecular Biology*. New York.
- Bartel, P.L., C. Chien, R. Sternglanz, and S. Fields. 1993. Using the two-hybrid system to detect protein–protein interaction. In *Cellular Interaction in Development: a Practical Approach*. D.A. Harley, editor. IRL Press at Oxford University Press, Oxford, United Kingdom. 153–179.
- Bohmann, K., J. Ferreira, N. Santama, K. Weis, and A.I. Lamond. 1995a. Molecular analysis of the coiled body. *J. Cell Sci.* 19:107–113.
- Bohmann, K., J.A. Ferreira, and A.I. Lamond. 1995b. Mutational analysis of p80 coilin indicates a functional interaction between coiled bodies and the nucleolus. *J. Cell Biol.* 131:817–831.
- Brasch, K., and R.L. Ochs. 1992. Nuclear bodies (NBs): a newly rediscovered organelle. *Exp. Cell Res.* 202:211–223.
- Breeden, L., and K. Nasmyth. 1985. Regulation of the yeast HO gene. *Cold Spring Harb. Symp. Quant. Biol.* 50:643–650.

- Carmo-Fonseca, M., J. Ferreira, and A.I. Lamond. 1993. Assembly of snRNP-containing coiled bodies is regulated in interphase and mitosis - Evidence that the coiled body is a kinetic nuclear structure. *J. Cell Biol.* 120:841-852.
- Chen, C., and H. Okyama. 1987. High-efficiency transformation of mammalian cells by plasmid DNA. *Mol. Cell. Biol.* 7:2745-2752.
- Chen, H.K., and N.H. Yeh. 1997. The nucleolar phosphoprotein P130 is a GTPase/ATPase with intrinsic property to form large complexes triggered by F^- and Mg^{2+} . *Biochem. Biophys. Res. Commun.* 230:370-375.
- Ferreira, J., and M. Carmo-Fonseca. 1995. The biogenesis of the coiled body during early mouse development. *Development.* 121:601-612.
- Fields, S., and O.K. Song. 1989. A novel genetic system to detect protein-protein interactions. *Nature.* 340:245-246.
- Fischer, U., J. Huber, W.C. Boelens, I.W. Mattaj, and R. Lührmann. 1995. The HIV-1 rev activation domain is a nuclear export signal that accesses an export pathway used by specific cellular RNAs. *Cell.* 82:475-483.
- Ganot, P., M. Caizergues-Ferrer, and T. Kiss. 1997. The family of box ACA small nucleolar RNAs is defined by an evolutionarily conserved secondary structure and ubiquitous sequence elements essential for RNA accumulation. *Genes Dev.* 11:941-956.
- Guarente, L. 1983. Yeast promoters and lacZ fusions designed to study expression of cloned genes in yeast. *Methods Enzymol.* 101:181-191.
- Hannon, G.J., D. Demetrick, and D. Beach. 1993. Isolation of the Rb-related p130 through its interaction with CDK2 and cyclins. *Genes Dev.* 7:2378-2391.
- Hardin, J.H., S.S. Spicer, and W.B. Greene. 1969. The paranucleolar structure, accessory body of Cajal, sex chromatin, and related structures in nuclei of rat trigeminal neurons: a cytochemical and ultrastructural study. *Anat. Rec.* 164:403-432.
- Hollenberg, S.M., R. Sternglanz, P.F. Cheng, and H. Weintraub. 1995. Identification of a new family of tissue-specific basic helix-loop-helix proteins with a two-hybrid system. *Mol. Cell. Biol.* 15:3813-3822.
- Jiménez-García, L.F., M.d.L. Segura-Valdez, R.L. Ochs, L.I. Rothblum, R. Hannan, and D.L. Spector. 1994. Nucleogenesis: U3 snRNA-containing prenucleolar bodies move to sites of active pre-rRNA transcription after mitosis. *Mol. Biol. Cell.* 5:955-966.
- Kalderon, D., W.D. Richardson, A.F. Markham, and A.E. Smith. 1984. Sequence requirements for nuclear location of simian virus-40 large-T antigen. *Nature.* 311:33-38.
- Kiss-László, Z., Y. Henry, J.-P. Bachellerie, M. Caizergues-Ferrer, and T. Kiss. 1996. Site-specific ribose methylation of preribosomal RNA: a novel function for small nucleolar RNAs. *Cell.* 85:1077-1088.
- Lafarga, M., M.T. Berciano, M.A. Andres, and P.S. Testillano. 1994. Effects of cycloheximide in the structural organization of the nucleolus and the coiled body in normal and stimulated supraoptic neurons of the rat. *J. Neurocytol.* 23:500-513.
- Lafarga, M., J.P. Hervas, M.C. Santa-Cruz, J. Villegas, and D. Crespo. 1983. The accessory body of Cajal in the neuronal nucleus. A light and electron microscopic approach. *Anat. Embryol.* 166:19-30.
- Lafontaine, D.L.J., C. Bousquet-Antonelli, Y. Henry, M. Caizergues-Ferrer, and D. Tollervy. 1998. The box H+ACA snoRNAs carry Cbf5p, the putative rRNA pseudouridine synthase. *Genes Dev.* 12:527-537.
- Lanford, R.E., and J.S. Butel. 1984. Construction and characterization of an SV40 mutant defective in nuclear transport of T antigen. *Cell.* 37:801-813.
- Lerner, E.A., M.R. Lerner, C.A. Janeway, and J.A. Steitz. 1981. Monoclonal antibodies to nucleic acid-containing cellular constituents: Probes for molecular biology and autoimmune disease. *Proc. Natl. Acad. Sci. USA.* 78:2737-2741.
- Li, D., U.T. Meier, G. Dobrowolska, and E.G. Krebs. 1997. Specific interaction between casein kinase 2 and the nucleolar protein Nopp140. *J. Biol. Chem.* 272:3773-3779.
- Lischwe, M.A., R.L. Ochs, R. Reddy, R.G. Cook, L.C. Yeoman, E.C. Tan, M. Reichlin, and H. Busch. 1985. Purification and partial characterization of a nucleolar scleroderma antigen (Mr = 34,000; pI, 8.5) rich in N^G , N^G -dimethylarginine. *J. Biol. Chem.* 260:14304-14310.
- Lyon, C.E., K. Bohmann, J. Sleeman, and A.I. Lamond. 1997. Inhibition of protein dephosphorylation results in the accumulation of splicing snRNPs and coiled bodies within the nucleolus. *Exp. Cell Res.* 230:84-93.
- Malatesta, M., C. Zancanaro, T.E. Martin, E.K.L. Chan, F. Amalric, R. Lührmann, P. Vogel, and S. Fakan. 1994. Is the coiled body involved in nucleolar functions. *Exp. Cell Res.* 211:415-419.
- Maniatis, T., E.F. Fritsch, and J. Sambrook. 1989. Molecular Cloning: A Laboratory Manual. Ford, N., C. Nolan, and M. Ferguson, editors. Cold Spring Harbor, NY.
- Matilla, A., B.T. Koshy, C.J. Cummings, T. Isobe, H.T. Orr, and H.Y. Zoghbi. 1997. The cerebellar leucine-rich acidic nuclear protein interacts with ataxin-1. *Nature.* 389:974-978.
- McCutchan, J.H., and J.S. Pagano. 1968. Enhancement of the infectivity of simian virus 40 deoxyribonucleic acid with diethyl aminoethyl-dextran. *J. Natl. Cancer Inst.* 41:351-357.
- Meier, U.T. 1996. Comparison of the rat nucleolar protein Nopp140 to its yeast homolog SRP40: Differential phosphorylation in vertebrates and yeast. *J. Biol. Chem.* 271:19376-19384.
- Meier, U.T., and G. Blobel. 1990. A nuclear localization signal binding protein in the nucleolus. *J. Cell Biol.* 111:2235-2245.
- Meier, U.T., and G. Blobel. 1992. Nopp140 shuttles on tracks between nucleolus and cytoplasm. *Cell.* 70:127-138.
- Meier, U.T., and G. Blobel. 1994. NAP57, a mammalian nucleolar protein with a putative homolog in yeast and bacteria. *J. Cell Biol.* 127:1505-1514.
- Misteli, T., J.F. Caceres, and D.L. Spector. 1997. The dynamics of a pre-mRNA splicing factor in living cells. *Nature.* 387:523-527.
- Monneron, A., and W. Bernhard. 1969. Fine structural organization of the interphase nucleus in some mammalian cells. *J. Ultrastruct. Res.* 27:266-288.
- Nicoloso, M., L.-H. Qu, B. Michot, and J.-P. Bachellerie. 1996. Intron-encoded, antisense small nucleolar RNAs: the characterization of nine novel species points to their direct role as guides for the 2'-O-ribose methylation of rRNAs. *J. Mol. Biol.* 260:178-195.
- Ochs, R.L., T.W. Stein, Jr., and E.M. Tan. 1994. Coiled bodies in the nucleolus of breast cancer cells. *J. Cell Sci.* 107:385-399.
- Pollard, K.M., E.K. Chan, B.J. Grant, K.F. Sullivan, E.M. Tan, and C.A. Glass. 1990. In vitro posttranslational modification of lamin B cloned from a human T-cell line. *Mol. Cell. Biol.* 10:2164-2175.
- Ramón y Cajal, S. 1903. Un sencillo método de coloración selectiva del retículo protoplasmático y sus efectos en los diversos órganos nerviosos de vertebrados e invertebrados. *Trab. Lab. Invest. Biol.* 2:129-221.
- Raska, I., L.E.C. Andrade, R.L. Ochs, E.K.L. Chan, C.-M. Chang, G. Roos, and E.M. Tan. 1991. Immunological and ultrastructural studies of the nuclear coiled body with autoimmune antibodies. *Exp. Cell Res.* 195:27-37.
- Raska, I., R.L. Ochs, L.E.C. Andrade, E.K.L. Chan, R. Burlingame, C. Peebles, D. Gruol, and E.M. Tan. 1990. Association between the nucleolus and the coiled body. *J. Struct. Biol.* 104:120-127.
- Rebelo, L., F. Almeida, C. Ramos, K. Bohmann, A.I. Lamond, and M. Carmo-Fonseca. 1996. The dynamics of coiled bodies in the nucleus of adenovirus-infected cells. *Mol. Biol. Cell.* 7:1137-1151.
- Reimer, G., K.M. Pollard, C.A. Penning, R.L. Ochs, M.A. Lischwe, H. Busch, and E.M. Tan. 1987. Monoclonal autoantibody from a (New Zealand black × New Zealand white)F1 mouse and some human scleroderma sera target an Mr 34,000 nucleolar protein of the U3 RNP particle. *Arthritis Rheum.* 30:793-800.
- Skinner, P.J., B.T. Koshy, C.J. Cummings, I.A. Klement, K. Helin, A. Servadio, H.Y. Zoghbi, and H.T. Orr. 1997. Ataxin-1 with an expanded glutamine tract alters nuclear matrix-associated structures. *Nature.* 389:971-974.
- Spector, D.L. 1993. Macromolecular domains within the cell nucleus. *Annu. Rev. Cell Biol.* 9:265-315.
- Strouboulis, J., and A. Wolffe. 1996. Functional compartmentalization of the nucleus. *J. Cell Sci.* 109:1991-2000.
- Tollervy, D., H. Lehtonen, R. Jansen, H. Kern, and E.C. Hurt. 1993. Temperature-sensitive mutations demonstrate roles for yeast fibrillar in pre-rRNA processing, pre-rRNA methylation, and ribosome assembly. *Cell.* 72:443-457.
- Wilson, I.A., H.L. Niman, R.A. Houghten, A.R. Chersonson, M.R. Connolly, and R.A. Lerner. 1984. The structure of an antigenic determinant in a protein. *Cell.* 37:767-778.
- Wu, Z., C. Murphy, and J.G. Gall. 1994. Human p80-coilin is targeted to sphere organelles in the amphibian germinal vesicle. *Mol. Biol. Cell.* 5:1119-1127.